Materials Science and Engineering A 442 (2006) 297-301.

Elasticity study on collective motion in metallic glasses

T. Takahashi, H. Tanimoto and H. Mizubayashi*
Institute of Materials Science, University of Tsukuba, Tsukuba, Ibaraki 305-8573, Japan

Abstract

The frequency (f) dependence, $E(\varepsilon_{t0}, f)$, and the strain amplitude (ε_t) dependence, $E(\varepsilon_t, f_0)$, of the dynamic Young's modulus in a-$Cu_{50}Ti_{50}$ (MMG), a-$Zr_{50}Cu_{50}$ (MMG) and a-$Zr_{55}Cu_{30}Al_{10}Ni_5$ (BMG) were investigated at room temperature by means of the vibrating reed method in the frequency range between 10^1 Hz and 10^4 Hz, where ε_{t0}~10^{-6}, f_0~10^2 Hz and MMG and BMG are abbreviations of marginal and bulk metallic glasses, respectively. The effect of passing direct-current (PEC) on $E(\varepsilon_{t0}, f_0)$ was also investigate. The strong decrease in $E(\varepsilon_{t0}, f)$ between 10^1 Hz and 10^4 Hz, the strong increase in $E(\varepsilon_t, f_0)$ with increasing ε_t below 0.2% and the net increase in $E(\varepsilon_{t0}, f_0)$ under PEC with the current density of 10^7 A/m^2 were commonly found, indicating that the resonant collective motions of many atoms were excited in metallic glasses. For a-$Zr_{50}Cu_{50}$ and a-$Zr_{55}Cu_{30}Al_{10}Ni_5$, the effective charge, Z^*, for the effects of PEC was found to be 10^5 and showed decrease with increasing f. The magnitudes of all the changes were similar among the metallic glasses, indicating that the correlation between the collective motions and the free volume contained in metallic glasses is not too strong. The underlying mechanism was discussed.

Keywords; metallic glasses, resonant collective motion, density fluctuation, free volume
*Corresponding author. E-mail address: mizubayashi@ims.tsukuba.ac.jp

1. Introduction

Finding of acceleration of thermal crystallization in metallic glasses by an electric current [1,2] was the beginning of observation for various phenomena associated with collective motions of many atoms in metallic glasses. The reported characteristic phenomena are an increase in the dynamic Young's modulus at low-temperatures [3] and a decrease in the crystallization temperature, T_x, by 10 to 20 K at elevated temperatures [4] by passing an electric direct-current (PEC) of 10^7 A/m^2, the homogeneous deformation [5] and the crystallization [6] at low temperatures induced by resonant electropulsing and the decrease in the dynamic Young's modulus in the frequency range between 10^2 Hz and 10^4 Hz [7]. The number of atoms in a collective motion responsible for such phenomena was estimated to the order of 10^4 atoms [3,4] which was attributed to the density and/or the chemical fluctuations existing in metallic glasses [8-10]. Recently, it was reported for several bulk metallic glasses (BMG) that ultrasound induced the rapid crystallization around the glass transition temperature, T_g, where enhancement of atomic diffusion by the stochastic resonance was claimed to take place [11-13]. The underlying mechanisms for these characteristic phenomena are not known yet, where one of the reasons is a lack of the experimental knowledge

concerned. In the present work, focused is the dynamic Young's modulus in BMG and that in marginal metallic glasses (MMG), where the knowledge on the relationship between the free volume and the dynamic Young's modulus can be expected because the free volume contained is considerably smaller in BMG than in MMG.

2. Experimental

Amorphous (*a*-) ribbon specimens of *a*-$Zr_{55}Cu_{30}Al_{10}Ni_5$ (BMG), *a*-$Zr_{50}Cu_{50}$ (MMG) and *a*-$Cu_{50}Ti_{50}$ (MMG) were prepared by the melt spinning method in a high-purity Ar gas atmosphere. Four side surfaces of a ribbon specimen were mechanically polished into the rectangular shape and the thickness and width of the polished specimens were about 20 μm and 0.7 mm respectively. The static Young's modulus, E_s, were measured by quasi-static tensile tests in the strain range below about 0.3 %, where specimens showed the linear elastic behavior. The dynamic Young's modulus, $E(\varepsilon_t,f)$, was measured as a function of the strain amplitude, ε_t, and the frequency, f, by means of the vibrating reed methods described in [7]. $E(\varepsilon_{t0},f)$ was measured as a function of the specimen length at ε_{t0} of 10^{-6} and $E(\varepsilon_t,f_0)$ was measured as a function of the vibrating amplitude at f_0 of ~100 Hz, respectively. A change in $E(\varepsilon_{t0},f_0)$ under PEC was measured as a function of the current density i_d at ε_{t0} of 10^{-6} and f_0 between ~10 and 1000 Hz, where the measurement setup was similar to that reported in [14].

3. Results

Figs. 1(a) to 1(c) show the Young's modulus data observed for *a*-$Zr_{55}Cu_{30}Al_{10}Ni_5$. For the quasi static tensile test (Fig. 1(a)), the linear elasticity was observed for ε_t below 0.5 %, where E_s of 97.5 GPa was determined as the mean value of four as prepared specimens. As seen in Fig. 1(b), $E(\varepsilon_{t0}, f)$ observed between 10 Hz and 10^3 Hz are considerably lower than E_s showing local minima, where the outline of $E(\varepsilon_{t0}, f)$ is similar among the specimens but the amount of decrease in $E(\varepsilon_{t0}, f)$ measured referred to E_s was variable among specimens. In Fig. 1(c), $E(\varepsilon_{t0}, f)$ and E_s observed for the specimens annealed at 570 K, 700 K and 850 K for 0.5 h are shown. In the X-ray diffraction (XRD) measurements (not shown here), no crystallization was detected after annealing at 570 K and 700 K but the fractional volume of about 70 % was crystallized after annealing at 850 K, respectively. E_s showed an increase with increasing annealing temperature. Referring to E_s, the $E(\varepsilon_{t0}, f)$ data observed after annealing at 570 K and 700 K were similar to those found for the as prepared specimens. In contrast, the $E(\varepsilon_{t0}, f)$ data observed after annealing at 850 K fell near E_s, indicating that the decrease in $E(\varepsilon_{t0}, f)$ is characteristic of metallic glasses. Figs. 2(a) and (b) show the $E(\varepsilon_{t0}, f)$ data observed for *a*-$Zr_{50}Cu_{50}$ and *a*-$Cu_{50}Ti_{50}$, respectively. Both the $E(\varepsilon_{t0}, f)$ data are similar to those for *a*-$Zr_{55}Cu_{30}Al_{10}Ni_5$ shown in Fig. 1(b).

Fig. 3 shows examples for the $(f/f_0)^2$ *vs.* ε_t data observed for *a*-$Zr_{55}Cu_{30}Al_{10}Ni_5$, *a*-$Zr_{50}Cu_{50}$ and *a*-$Cu_{50}Ti_{50}$, where $E(\varepsilon_t, f_0)/E(\varepsilon_{t0}, f_0) \sim (f/f_0)^2$. With increasing ε_t, $(f/f_0)^2$ showed an increase followed by saturation. The out line of the $(f/f_0)^2$ *vs.* ε_t data observed for *a*-$Zr_{55}Cu_{30}Al_{10}Ni_5$, *a*-$Zr_{50}Cu_{50}$ and *a*-$Cu_{50}Ti_{50}$ were very similar to that already reported [15] except that the amounts of the increases in $(f/f_0)^2$ observed in the present *a*-$Zr_{50}Cu_{50}$ and *a*-$Cu_{50}Ti_{50}$ specimens were about 60 % of those in the *a*-$Zr_{50}Cu_{50}$ and *a*-$Cu_{50}Ti_{50}$ specimens used in [15]. A change in $E(\varepsilon_{t0},f_0)$ under PEC with $i_d \sim 10^7$ A/m^2 was measured in a He gas atmosphere of about 0.1 atm in order to minimize an increase in the specimen temperature due to joule heating [14]. Fig. 4 shows an example of a change in the temperature along the specimen long

axis, ΔT_x, observed during resonant vibrations of a reed specimen of *a*-$Zr_{50}Cu_{50}$ under PEC. The observed ΔT_x *vs*. distance, *x*, data reflect the experimental setup that the specimen was clamped at $x=0$ and thermally anchored at the specimen top of $x=L$ by a thin copper lead ribbon. The dashed line denotes the relative change in strain, $\varepsilon_x/\varepsilon_0$, estimated from the vibration shape [16]. Fig. 5(a) shows the observed change in *f* as a function of i_d and the estimated change in *f* due to joule heating which was evaluated from using the ΔT_x data, $\varepsilon_x/\varepsilon_0$ and the temperature change in *f* measured separately without PEC. The intrinsic change in *f*, Δf_{PEC}, due to PEC was determined as shown in Fig. 5(a). Fig. 5(b) shows $\Delta f_{PEC}/f_0$ as a function of i_d and the $\Delta f/f_0$ *vs*. ε_t deduced from the $(f/f_0)^2$ *vs*. ε_t data shown in Fig. 3. They were compared by assuming the scaling relationship, $\varepsilon_t = \alpha\, i_d$, between i_d and ε_t with a proportional constant, α. The scaling assumed that the electromigration force acting to an atom was the same to the elastic force acting to an atom under stress, giving the relationship,

$$Z^* = \alpha\, S\, E/e\rho_{\mathrm{R}}, \qquad (1)$$

where Z^*, *S*, *e* and ρ_R denote the effective charge number, a dimensional cross-section of an atom, the elementary charge and the specific resistivity of the a-alloy, respectively (see [14,17] for details). Figs. 6(a) and (b) show the Z^* *vs*. *f* data found for *a*-$Zr_{50}Cu_{50}$ together with that reported [17] and for *a*-$Zr_{55}Cu_{30}Al_{10}Ni_5$, respectively. For both *a*-$Zr_{50}Cu_{50}$ and *a*-$Zr_{55}Cu_{30}Al_{10}Ni_5$, Z^* was in the order of 10^5 in the frequency range between 50 Hz and 1000 Hz and showed a decrease with increasing *f*.

4. Discussion

Fig. 7 shows the schematic drawing for the strain and frequency dependence of the Young's modulus of metallic glasses reported in [7,14], where E_s,. $E(\varepsilon_{t0}, f)$ and $E(\varepsilon_t, f_0)$ are depicted by the line AB, the curve ACD and the curve CE, respectively. Computer simulation works on metallic glass [18,19] have shown that the amorphous structure is composed of the relatively lower dense region (RLDR) and the relatively higher dense region (RHDR). It is suggested that the reversible shear deformation of small deformable units in the RLDR is responsible for the much lower E_s in the amorphous state compared with that in the crystalline state [19]. For *a*-$Zr_{55}Cu_{30}Al_{10}Ni_5$, the constituent anelastic strain, ε_a, in ε_t for the quasi static tensile tests was estimated as about 0.25 in the ratio $\varepsilon_a/\varepsilon_t$ from the E_s data shown in Fig. 1(c). For the decreased $E(\varepsilon_{t0}, f)$ observed between 10 Hz and 10^3 Hz shown in Fig. 1(b), $\varepsilon_a/\varepsilon_t$ estimated was about 0.4, indicating a strong increase in ε_a. In order to explain such strong increase in ε_a, the resonant collective motion of the RHDR embedded in the RLDR will be discussed below.

For the forced vibration of resonant systems with the mass, *m*, the dependence of the displacement amplitude, x_0, on the angular frequency, ω, can be given by

$$x_0^2 = (F_0/m)^2/[(\omega^2 - \omega_r^2)^2 + \omega_r^4 \tan^2\phi], \qquad (2)$$

where F_0 is the strength of a periodic applied force, ω_r is the resonant angular frequency and ϕ is the loss angle [16]. Then, we assume that ε_a, is explained by,

$$\varepsilon_a = \beta/[(\omega^2 - \omega_r^2)^2 + \omega_r^4 \tan^2\phi]^{1/2}, \qquad (3)$$

and $E(\varepsilon_{t0}, f)$ is given by,

$$E(\varepsilon_{t0}, f) = E_s [\varepsilon_0 /(\varepsilon_0 + \varepsilon_a)], \quad (4)$$

where ε_0 is the elastic strain and β is a proportional constant. For the resonant collective motion of RHDR, $\tan\phi$ may be considerably large because the RHDR is embedded in the RLDR. For such case, the dependence of ε_a on ω is not strongly modified by a change in $\tan\phi$. Dashed curves shown in Figs. 1(b), 2(a) and 2(b) were the theoretical values of $E(\varepsilon_{t0}, f)$ fitted to the observed data, where $\tan^2\phi$ was assumed to be 0.5 and the ω_r data used were those found in the electropulsing-induced crystallization on *a*-$Cu_{50}Ti_{50}$ [6] and *a*-$Zr_{50}Cu_{50}$ and *a*-$Zr_{55}Cu_{30}Al_{10}Ni_5$ (not shown here). For *a*-$Cu_{50}Ti_{50}$ shown in Fig. 2(b), the theoretical values of $E(\varepsilon_{t0}, f)$ explained well the observed data. For *a*-$Zr_{50}Cu_{50}$ and *a*-$Zr_{55}Cu_{30}Al_{10}Ni_5$, although the ω_r data are limited at present, but the theoretical values of $E(\varepsilon_{t0}, f)$ appeared to explain well the observed data too.

For $E(\varepsilon_t, f_0)$ shown in Fig. 3 and the curve CE in Fig. 7, the saturation in the reversible shear deformation of small deformable units [20] can be explained them. Then, one may expect the similar change in $E(\varepsilon_{t0}, f_0)$ at ε_{t0}.of 10^{-6} when the concentration of the electromigration force takes place through a collective motion of many atoms. The net increase in $E(\varepsilon_{t0}, f_0)$ under PEC as seen in Fig. 5(a) is indicative of the concentration of the electromigration force, where Z^* is indicative of the number of atoms associated with the collective motion. As shown in Figs. 6(a) and 6(b), for both *a*-$Zr_{50}Cu_{50}$ and *a*-$Zr_{55}Cu_{30}Al_{10}Ni_5$, Z^* was in the order of 10^5 and showed a decrease with increasing *f*. It is noted that the present value of Z^* is larger by four to five digits than the electromigration charge number of a single atom in a concentrated alloy [21]. The decrease in Z^* with increasing *f* may indicates that the number of atoms in the RHDR associated with the resonant collective motions decrease with increasing resonant frequency.

It is known that the free volume existing in BMG is considerably smaller than that in MMG. It is not for the free volume but the crystallization volume reported is 0.8 % for *a*-$Cu_{50}Ti_{50}$ [22], 2.1 % for *a*-$Zr_{50}Cu_{50}$ [23] and 0.4 % for *a*-$Zr_{55}Cu_{30}Al_{10}Ni_5$ [24], respectively. On the other hand, the magnitudes of various anelastic responses for $E(\varepsilon_{t0}, f)$ and $E(\varepsilon_t, f_0)$ were very similar among these metallic glasses, indicating that the correlation between the present characteristic anelastic phenomena and the free volume in metallic glasses is not too strong. Further speculation is premature at present, however, the present work demonstrated characteristics of collective motions of many atoms in metallic glasses.

5. Conclusion

The elastic properties associated with the collective motion of many atoms in *a*-$Cu_{50}Ti_{50}$ (MMG), *a*-$Zr_{50}Cu_{50}$ (MMG) and *a*-$Zr_{55}Cu_{30}Al_{10}Ni_5$ (BMG) were investigated. The magnitudes of the anelastic responses for $E(\varepsilon_{t0}, f)$ and $E(\varepsilon_t, f_0)$ and the effective charge number Z^* for the effect of PEC on $E(\varepsilon_{t0}, f_0)$ were found to be similar among these metallic glasses indicating that the correlation between the present characteristic anelastic phenomena and the free volume in metallic glasses is not too strong. The decrease in Z^* with increasing *f* was found, indicating that the number of atoms in the RHDR associated with the resonant collective motions decrease with increasing resonant frequency. The underlying mechanism was discussed in the light of excitation of the resonant collective motions in metallic glasses.

Acknowledgement

This work is partly supported by a Grant in Aid for Scientific Research and the 21st Century Center of Excellence Program from the Ministry of Education, Culture, Sports, Science and Technology, Japan.

References

[1] H. Mizubayashi and S. Okuda, Phys. Rev. B 40 (1989) 8057.
[2] Z.H. Lai, H. Conrad, Y.S. Chao, S.Q. Wang and J. Sun, Scripta Metall. 23 (1989) 305.
[3] H. Mizubayashi and R. Takemoto, J. Alloys and Compd. 211/212 (1994) 340.
[4] R. Takemoto and H. Mizubayashi, Acta Metall. Mater. 43 (1995) 1495.
[5] H. Mizubayashi and T. Okamoto, Mater. Sci. Forum, 304-306 (1999) 355.
[6] H. Mizubayashi, N. Kameyama, T. Hao and H. Tanimoto, Phys. Rev. B 64 (2001) 054201.
[7] H. Mizubayashi, T. Okamoto, K. Koyama and M. Horiuchi, Acta Mater. 46 (1998) 1257.
[8] K. Maeda, S. Takeuchi, J. Phys. F : Met. Pys. 12 (1982) 2767.
[9] J.-B. Suck, J. Non-cryst. Solids 293-295 (2001) 370
[10] A.S. Bakai, V.V. Kul'ko, I.M.Mikhailovskij, V.B. Rabukhin, O.A. Velikodnaya, J. Non-cryst. Solids.182 (1995) 315.
[11] T. Ichitsubo, S. Kai, H. Ogi, M. Hirao and K. Tanaka, Scripta Mater. 49 (2003) 267.
[12] T. Ichitsubo, E. Matsubara, S. Kai, and M. Hirao, Acta Mater. 52 (2004) 423.
[13] T. Ichitsubo, E. Matsubara, K. Anazawa, N. Nishiyama, S. Kai, and M. Hirao, Mater. Trans. JIM 45 (2004) 1189.
[14] H. Mizubayashi, T. Usui, H. Tanimoto, Mater. Sci. Engng. A 370 (2004) 260.
[15] H. Mizubayashi, T. Usui, H. Tanimoto, J. Non-cryst. Solids 312-314 (2002) 542.
[16] A.S. Nowick and B.S. Berry, *Anelastic Relaxation in Crystalline Solids* (Academic Press, New York, 1972) p. 15 and p. 626.
[17] R. Takemoto, M. Nagata and H. Mizubayashi, Acta Metall. Mater. 44 (1996) 2787.
[18] D. Weaire, M.F. Ashby, J. Logan and M.J. Weins, Acta Metall. 19 (1971) 779.
[19] S. Takeuchi and K. Maeda, Key Engineering Materials 13/15 (1987) 749.
[20] Y. Suzuki, J. Haimovich, and T. Egami, Phys. Rev. B 35 (1987) 2162.
[21] H.B. Huntington, *Diffusion in Solids*, ed. A.S. Nowic and J.J.Burton (Academic Press, New York, 1975), p.303.
[22] H. Mizubayashi, S. Hoshina and S. Okuda, J. Non-Crystalline Solids 117/118 (1990) 203.
[23] H. Mizubayashi, M. Kaida, S. Otsuka and S. Okuda, Acta Mater. 42 (1994) 2099.
[24] A. Inoue, Acta Mater. 48 (2000) 279.

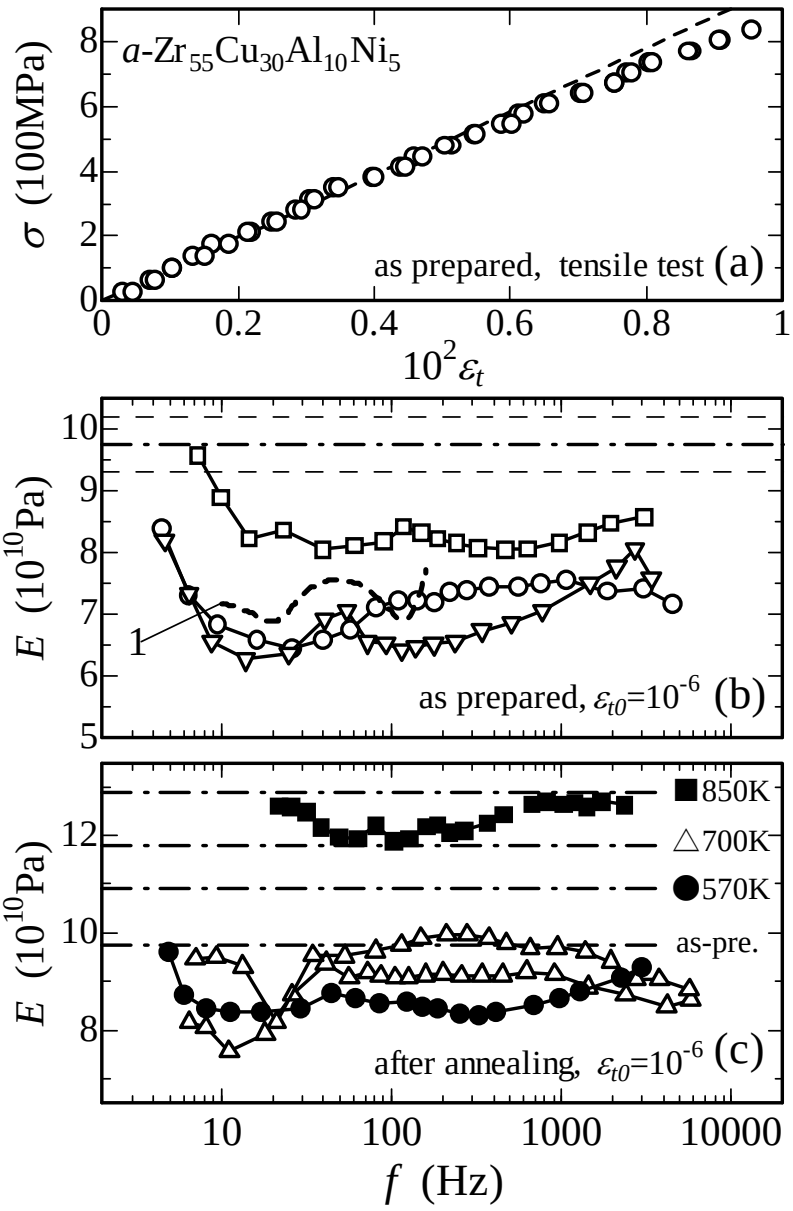

Fig. 1.

The Young's modulus data observed for *a*-$Zr_{55}Cu_{30}Al_{10}Ni_5$. (a) An example of the quasi static tensile test for an as prepared specimen, where the dashed line denotes the linear elasticity with E_s of 97.5 GPa which was the mean value of four specimens (not shown here). (b) Examples of $E(\varepsilon_{t0}, f)$ observed with $\varepsilon_{t0}=10^{-6}$ for three as-prepared specimens (symbols). The dash and dotted line denotes E_s mentioned above and two dashed lines denote the range in which the E_s data were found. (c) Similar to (b) but here shown are the $E(\varepsilon_{t0}, f)$ data (●) and E_s observed for the specimen after annealing at 570 K for 0.5 h, the $E(\varepsilon_{t0}, f)$ data (△) and E_s observed for the two specimens after annealing at 700 K for 0.5 h and the $E(\varepsilon_{t0}, f)$ data (■) and E_s observed for the specimen after annealing at 850 K for 0.5 h. See text for the dashed curve 1 in (b).

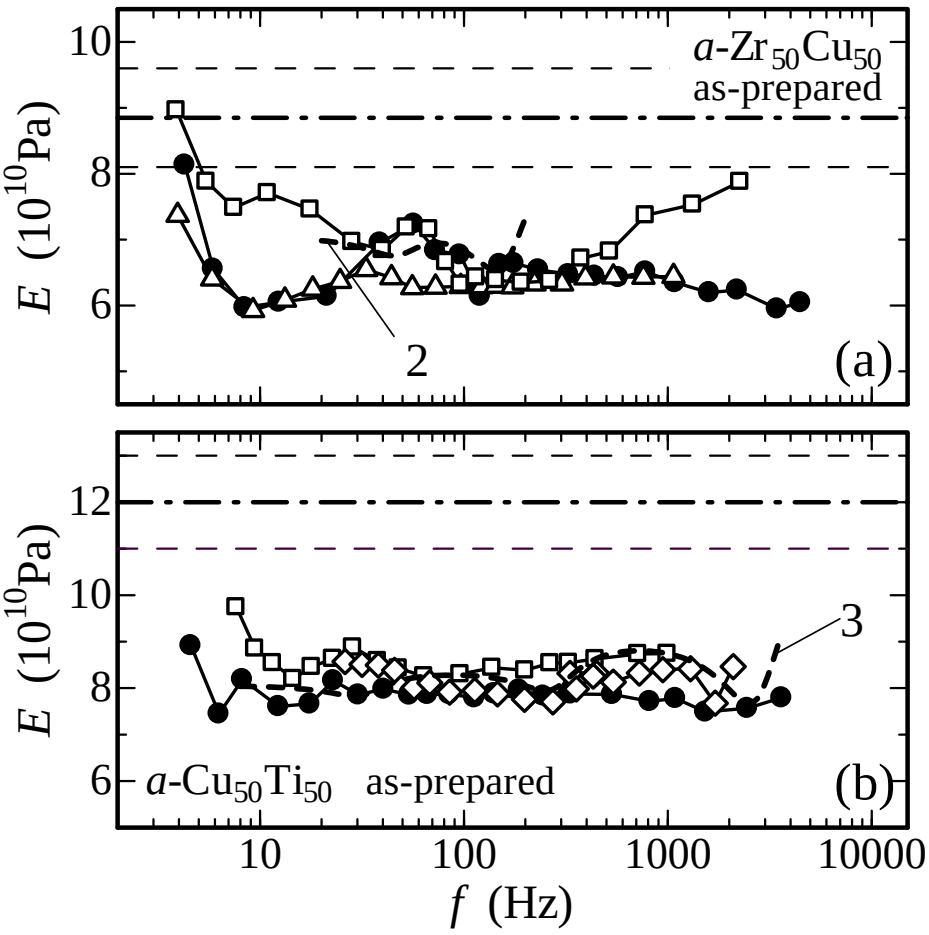

Fig. 2.

Similar to Fig. 1(b) but here the $E(\varepsilon_{t0}, f)$ data observed for (a) three as prepared specimens of a-$Zr_{50}Cu_{50}$ and (b) three as prepared specimens of a-$Cu_{50}Ti_{50}$. See text for the dashed curve 2 and 3.

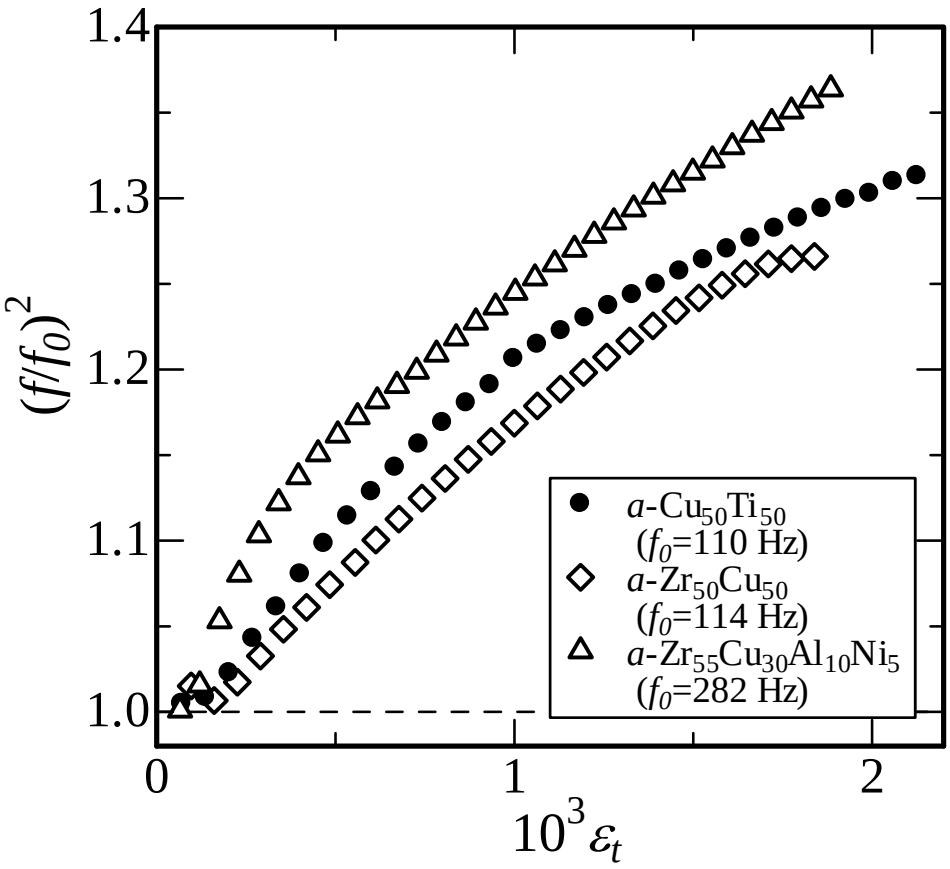

Fig. 3.

Examples for the $(f/f_0)^2$ *vs.* ε_t data observed for a-$Zr_{55}Cu_{30}Al_{10}Ni_5$, a-$Zr_{50}Cu_{50}$ and a-$Cu_{50}Ti_{50}$.

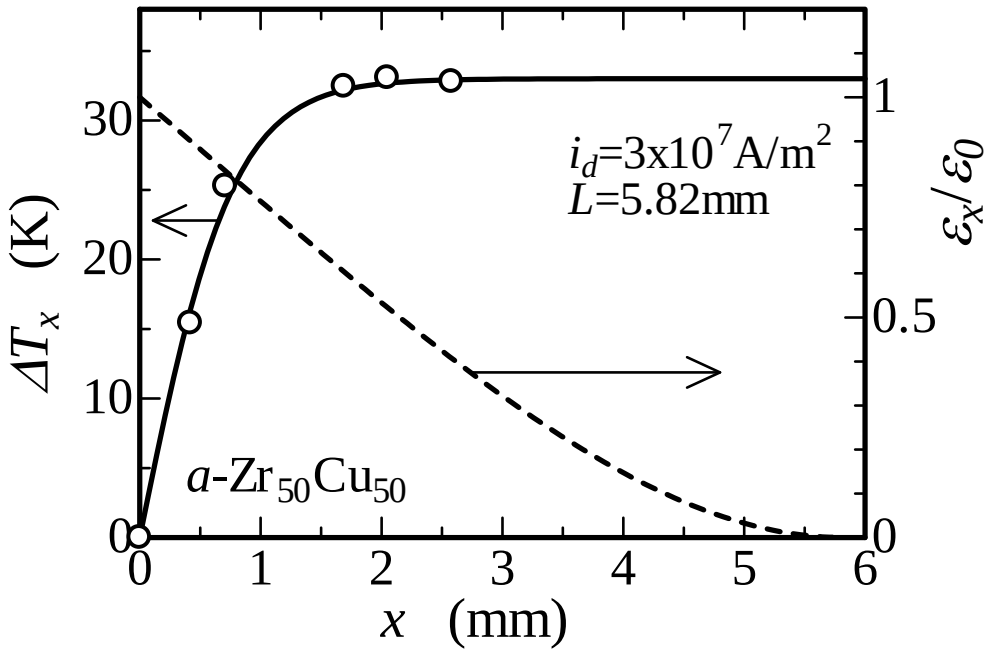

Fig. 4.
An example of a change in the temperature along the specimen long axis, ΔT_x, during PEC with i_d=3.0x10^7 A/m^2 observed for an a-$Zr_{50}Cu_{50}$ specimen (○). The dashed line denotes the relative change in strain, $\varepsilon_x/\varepsilon_0$, estimated from the vibration shape [16].

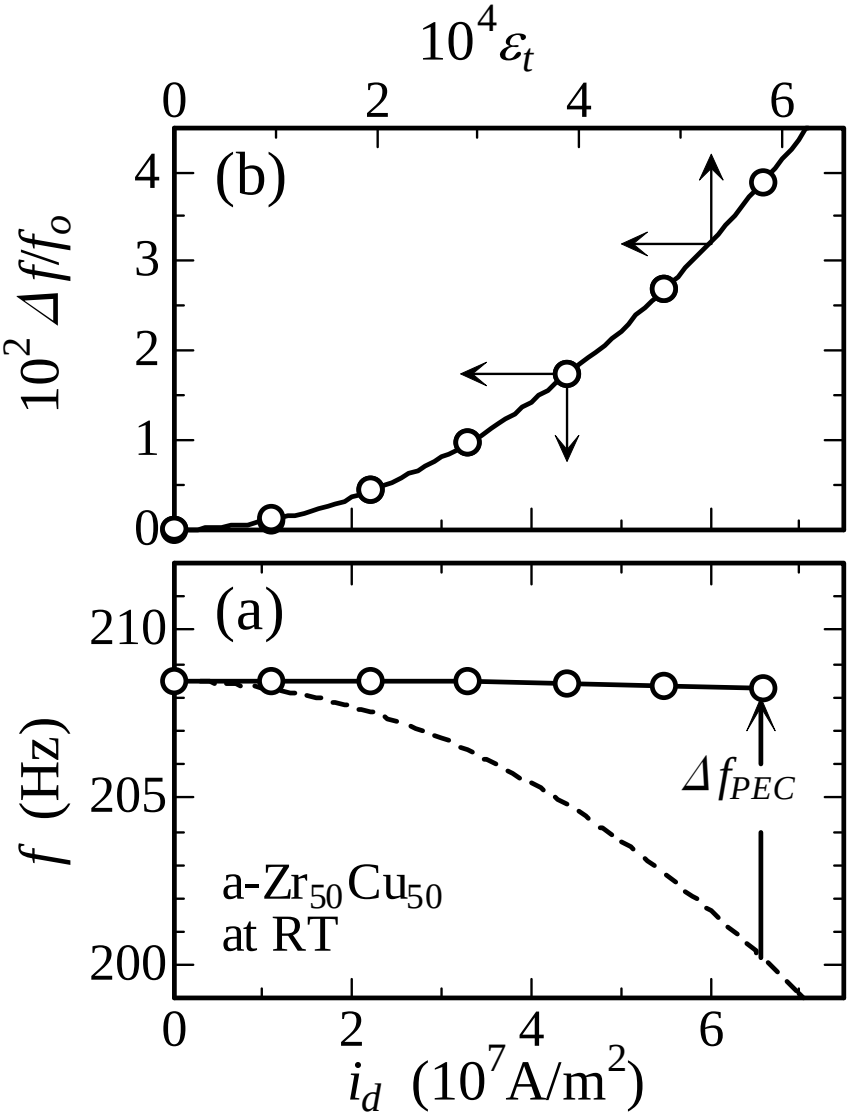

Fig. 5.
An example of a change in $E(\varepsilon_{t0},f_0)$ under PEC observed for *a*-$Zr_{50}Cu_{50}$. (a) The *f vs.* i_d data (○) and the change in *f* due to the joule heating (the dashed curve), where the net effect of PEC on *f*, Δf_{PEC}, was determined as shown in the figure. (b) The $\Delta f_{PEC}/f_0$ *vs.* i_d data (○) was compared with the f/f_0 *vs.* ε_t data shown in Fig. 3 (the solid curve) after scaling them. See text for details.

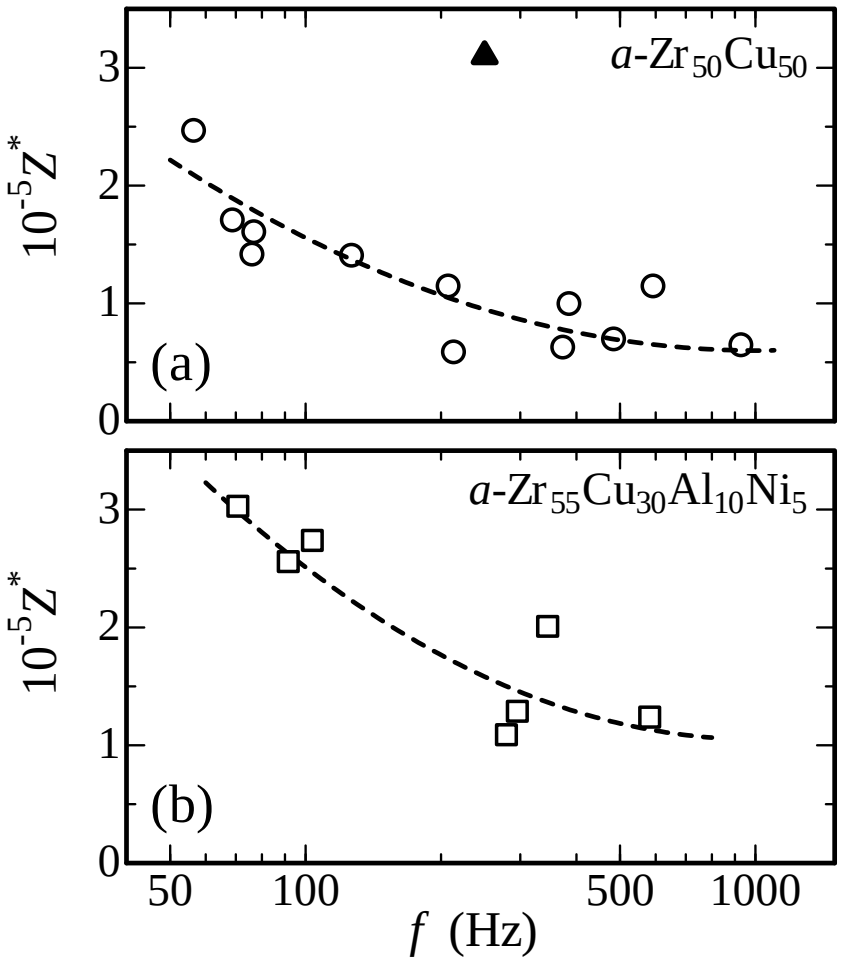

Fig. 6.
The Z^* *vs*. f data found for (a) *a*-$Zr_{50}Cu_{50}$ (○) together with that reported (▲) [17] and (b) *a*-$Zr_{55}Cu_{30}Al_{10}Ni_5$ (□). Dashed curves are drawn to guide eyes.

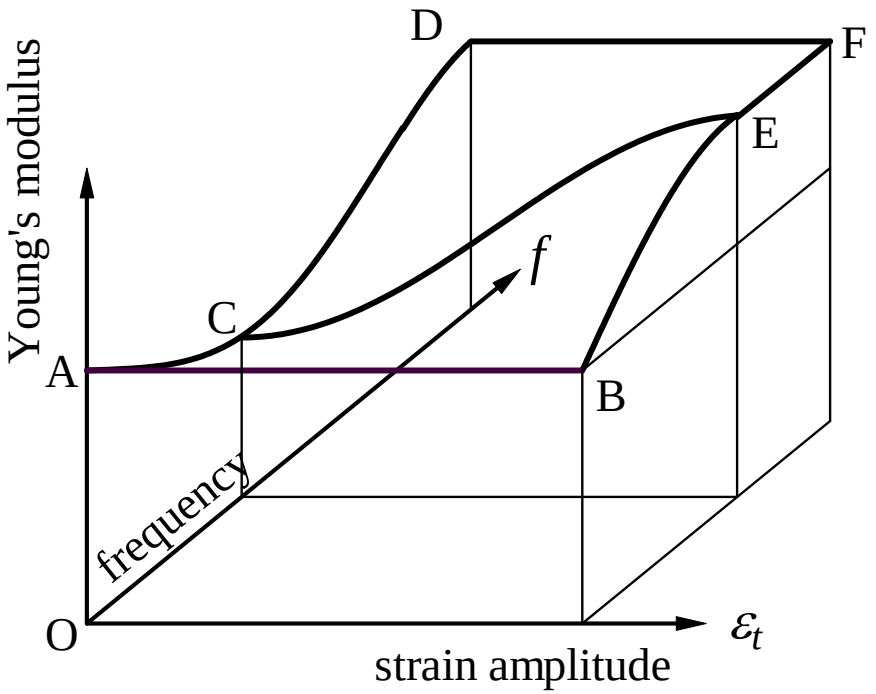

Fig. 7.
The schematic drawing for the strain and frequency dependence of the Young's modulus of metallic glasses [7,14].